Hybrid Graphene Oxide Based Ultrasensitive SERS Probe for Label-Free Biosensing

ARTICLE *in* JOURNAL OF PHYSICAL CHEMISTRY LETTERS · OCTOBER 2013

Impact Factor: 7.46 · DOI: 10.1021/jz4020597

3 AUTHORS, INCLUDING:

Rajashekhar Kanchanapally
Jackson State University
20 PUBLICATIONS **207** CITATIONS

THE JOURNAL OF PHYSICAL CHEMISTRY Letters

Letter

pubs.acs.org/JPCL

Hybrid Graphene Oxide Based Ultrasensitive SERS Probe for Label-Free Biosensing

Zhen Fan, Rajashekhar Kanchanapally, and Paresh Chandra Ray*

Department of Chemistry and Biochemistry, Jackson State University, Jackson, Mississippi, United States

Supporting Information

ABSTRACT: A metal nanoparticle attached to graphene oxide has the ability to open a new avenue of research with significant opportunities in the biomedical field. In this Letter, we report graphene oxide attached to a popcorn-shaped gold nanoparticle based hybrid SERS probe with ultrasensitive label-free sensing of HIV DNA and bacteria and provide its chemical fingerprint. Our SERS data with the hybrid material shows that it can be used for label-free detection of HIV DNA on the femto-molar level without any labeling. Experimental data with a novel SERS substrate show excellent reproducibility of the SERS signal. The current Letter demonstrates that the label-free SERS detection limit using a hybrid material can be as low as 10 CFU/mL for MRSA bacteria. The possible mechanism for very high sensitivity has been discussed.

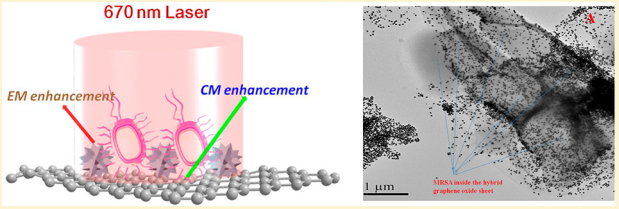

SECTION: Plasmonics, Optical Materials, and Hard Matter

Development of highly sensitive biosensing technologies that have the ability to shift medical diagnoses to the next level will have numerous applications, including the detection of DNA/RNA or an antigen/antibody for the measurement of clinical parameters, pathogens, and circulating tumor cells.[1−8] Surface-enhanced Raman spectroscopy (SERS) has been shown to be highly promising for biosensing applications due its ability to enhance Raman signals by factors up to 10^6−10^{14} orders of magnitude with the potential for single-molecule detection and featuring the specificity due to its unique molecular fingerprinting information.[9−18] SERS is highly promising for medical diagnosis and monitoring of diseases[19−23] because of their high sensitivity, label-free detection capability, low sample volumes, low-cost instruments, and real-time detection.[24−28] The human immunodeficiency virus (HIV) infections are one of the leading killers in Africa, Asia, and the Middle East.[3,4] On the other hand, methicillin-resistant *Staphylococcus aureus* (MRSA) infections in the U.S. are approximately 100 000/year, with 20 000 lives lost.[5−7] Driven by the need, in this Letter, we report a graphene oxide attached popcorn-shaped gold nanoparticle based hybrid SERS probe with ultrasensitive HIV DNA and MRSA capability.

Graphene oxide is chemically treated graphene and has most recently emerged as a potential alternative to graphene.[29−38] Graphene oxide is considered as a promising material for biological applications owing to its excellent aqueous processing ability, amphiphilicity, surface functionalizing ability, and fluorescence quenching ability.[39−49] Recently, it has been reported that graphene oxide can provide a SERS platform for studying the chemical (CM) enhancement, where Raman-active molecule−graphene interaction controls the magnitude of Raman enhancement.[28−35] Because the surface plasmon on graphene is in the terahertz range, scientists believe that graphene oxide will not support electromagnetic (EM) enhancement for SERS, as reported before.[28−34] Because an excellent SERS probe should possess strong electromagnetic and chemical enhancement capability for providing enough sensitivity, here, we have constructed a novel SERS probe with ultrasensitive sensing capability, based on a plasmonic nanopopcorn conjugated graphene oxide, as shown in Figure 1. To demonstrate that the SERS probe designed by us is versatile for biological analysis, we have shown that the novel SERS probe can be used for ultraselective label-free SERS sensing of HIV DNA and MRSA bacteria.

A novel SERS probe based on graphene oxide attached to nanopopcorn was synthesized via a four-step process, as shown in Figure 1. The detailed synthesis procedure and characterization are discussed in the Supporting Information. In the hybrid graphene oxide based SERS probe, due to the presence of a large surface area and very high aspect ratio, graphene oxide will be useful as a flat SERS substrate. It will enhance the Raman signal via a chemical enhancement mechanism. On the other hand, in nanopopcorn, due to the presence of tips, the SERS enhancement from nanopopcorn can arise from a combination lightning rod effect[48] and surface plasmon excitations,[22,23] as we have reported before. Also in our design of hybrid graphene oxide, the nanopopcorn also can be used as reactive sites for the binding with particular DNA or bacteria selectively. To understand the SERS signal enhancement capability of our developed graphene oxide based hybrid SERS substrate, we have used well-characterized Raman-active Rh6G dyes at different concentrations.

Received: September 24, 2013
Accepted: October 28, 2013
Published: October 28, 2013

   dx.doi.org/10.1021/jz4020597 | *J. Phys. Chem. Lett.* 2013, 4, 3813−3818

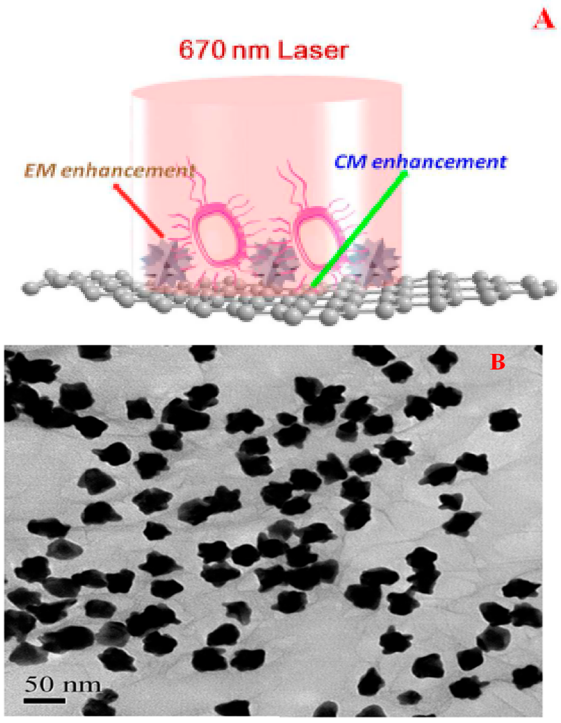

Figure 1. (A) The schematic representation shows a hybrid graphene oxide based SERS probe for tuning electromagnetic and chemical enhancement simultaneously to detect MRSA. (B) The TEM picture shows the morphology of the hybrid graphene oxide, where graphene oxide has been attached to nanopopcorn.

As shown in Figure 2A, we see very nice SERS spectra from 10^{-10} M Rh6G adsorbed on nanoassemblies. On the other hand, SERS spectra from 10^{-2} M Rh6G adsorbed on graphene oxide are almost negligible. The observed Raman modes from Rh6G at 615, 778, 1181, 1349 1366, 1511, 1570, 1603, and 1650 cm^{-1} are due to the vibration of C−C−C ring in-plane bending, C−H out-of-plane bending, C−N stretching, and C−C stretching, as reported by several groups including ours.[20−27] It seems like the Rh6G Raman bands at 1349 and 1598 cm^{-1} are combined with the D and G bands of graphene oxide. The Raman enhancement, G, is measured experimentally by direct comparison, as shown below[20−27]

$$G = \frac{[I_{SERS}]}{[I_{Raman}]} \times \frac{[M_{bulk}]}{[M_{ads}]} \quad (1)$$

where I_{SERS} is the intensity of a 1511 cm^{-1} vibrational mode in the surface-enhanced spectrum in the presence of graphene oxide, nanopopcorn, or hybrid graphene oxide and I_{Raman} is the intensity of the same mode in the bulk Raman spectrum from only Rh6G. M_{bulk} is the number of molecules used in the bulk, and M_{ads} is the number of molecules adsorbed on the nanosurface. All spectra were normalized for integration time using Ocean Optics software. From the SERS signal and normal Raman signal ratio for the 1511 cm^{-1} band, we have estimated that the enhancement factors are approximately 3.8×10^{11} in the case of nanoassemblies, 1.2×10^{9} for gold nanopopcorn, and 1.7×10^{2} for graphene oxide at 670 nm excitation. Our experimental data indicated no significant changes in Raman frequencies of Rh6G in SERS and Raman bands.

It is really interesting to note from Figure 2 that only graphene oxide can be used for Raman enhancement by 2

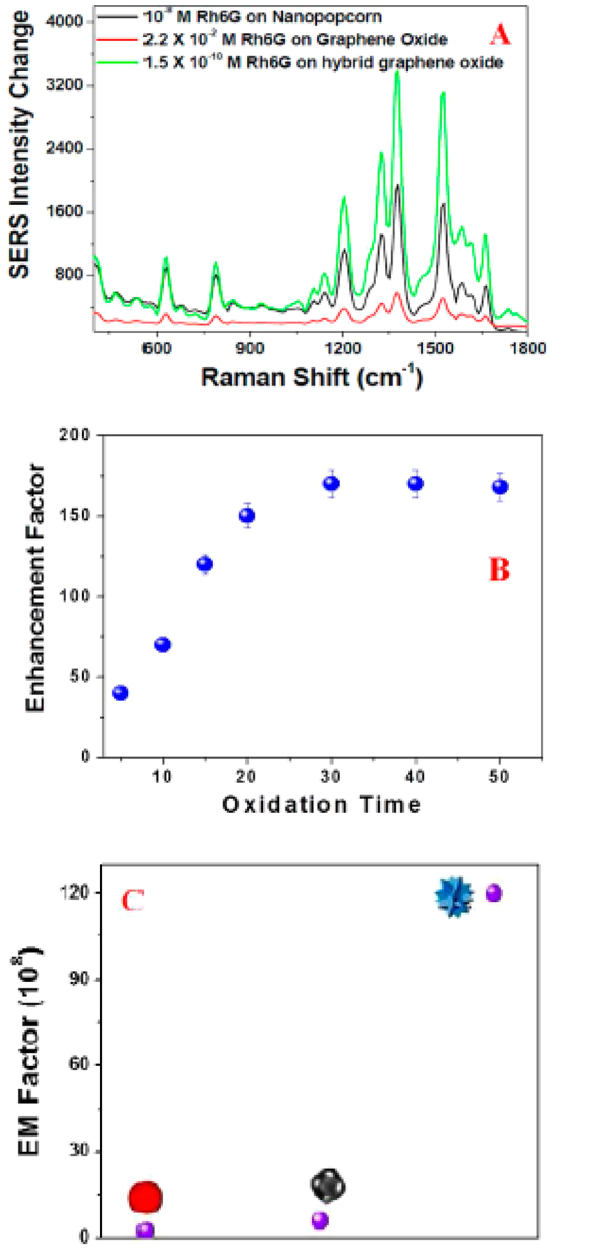

Figure 2. (A) Plot showing SERS enhancement of the Raman signal at 785 nm excitation from Rh6G, in the presence of graphene oxide, gold nanopopcorn, and a nanopopcorn-attached graphene oxide hybrid. (B) Plot showing how the chemical enhancement factor varies with the oxidation time of graphene oxide. (C) Plot showing how the EM enhancement factor varies with the shape of the nanoparticle.

orders of magnitude. Because the surface plasmon on graphene is in the terahertz range, our observed SERS enhancement by 2 orders of magnitude is mainly due to the chemical enhancement. During the oxidation treatment, graphene oxide possesses active oxygen sites, which can interact with Rh6G. We believe that the impacts of chemical interaction between Rh6G and oxygen sites as well as the global π-conjugation network are responsible for the chemical enhancement of SERS. Next, to understand how the chemical enhancement factor is influenced by the oxidation treatment time, we have performed a SERS experiment using nanomaterials prepared at different oxidation treatment times. As one can see from Figure 2B, the SERS enhancement factor increases with oxidation time

dx.doi.org/10.1021/jz4020597 | J. Phys. Chem. Lett. 2013, 4, 3813−3818

until 30 min of oxidation, and it is mainly due to the formation of more active oxygen sites during the oxidation process. Our experimental data show that the enhancement factor is about 1.2×10^9 in the case of gold nanopopcorn, and this huge SERS enhancement in the case of nanopopcorn is mainly due to the electromagnetic enhancement and a lighting rod effect, as we have reported before. As shown in Figure 2, we have observed a 3.8×10^{11} SERS enhancement factor for the hybrid material. This huge SERS enhancement in the hybrid material is mainly due to the chemical enhancement by graphene oxide and very high plasmon enhancement by nanopopcorn.

Next, to understand how the SERS enhancement factor for hybrid materials varies with the shape of the gold nanoparticles, we have measured the SERS enhancement factor for hybrid graphene oxide made with spherical-, cage-, and popcorn-shaped nanoparticles. Our experimental results indicate that the enhancement factor is about 7.6×10^9 for a spherical gold nanoparticle attached to hybrid graphene oxide. On the other hand, the SERS enhancement factor is about 3×10^{10} for the cage-shaped nanoparticle attached to graphene oxide, where the SERS enhancement factor is about 3.8×10^{11} in the case of the nanopopcorn-attached hybrid graphene oxide. Next, to understand the shape-dependent SERS enhancement factor, we have also measured the SERS enhancement factor for gold naparticles of different shape without graphene oxide. As shown in Figure 2C, our experimental data show that the EM enhancement factor is about 50 times higher for star-shaped nanopopcorn than the spherical nanoparticle, and it is due to the presence of sharp tips on the nanopopcorn, as we discussed before. All of the above data clearly show that the chemical enhancement factor is about 10^2 for hybrid graphene oxide; on the other hand, the plasmon enhancement factor varies from 2×10^7 to 10^9, depending on the shape of the gold nanoparticles.

Next, to found out whether the hybrid graphene oxide based SERS probe can be used for the sensitive label-free detection of DNA, we have tested for the detection of HIV DNA. Because certain regions of the gag-gene, such as p24, are highly conserved among HIV isolates, many therapeutic strategies have been directed at gag-gene targets.[3,4] We therefore used a segment of the HIV gag-gene sequence as a target DNA. To demonstrate that the SERS assay can be used for HIV DNA detection, we used initially a partial sequence of the HIV-1 gag-gene, 5′-AGAAGATATTTGGAATAACAT-3′-SH, as the probe DNA. Figure 3A shows the SERS spectra for DNA, where one can see the dominance of the adenine ring stretching modes at 736 cm^{-1}. All SERS bands can be assigned easily with the literature-reported data for DNA,[12−16] as shown in Table 1. The SERS signal from the adenine bases appears to be more greatly enhanced than that of the other DNA bases. The band at 1098 cm^{-1} is mainly due to the phosphate backbone. Observed SERS bands at 1300 and 1360 $cm^{-1}$are due to the ring breathing and stretching modes for thymine and cytosine. As shown in Figure 3A, the DNA SERS bands at 1360 and 1640 cm^{-1} are combined with the D and G bands of graphene oxide. To undestand whether the hyrid SERS probe is more superior than the only gold nanoparticle probe, we have performed the SERS experiment with different probes. Figure 3A clearly shows that the hybrid graphene oxide based SERS probe is around 2 orders of magnitude more sensitive than the only gold nanoparticle, and it is due to the availability of tuning both the EM and CM effects simultaneously. As we have discussed before, reproducibility and stability of SERS signals from a SERS-active probe are very important properties for

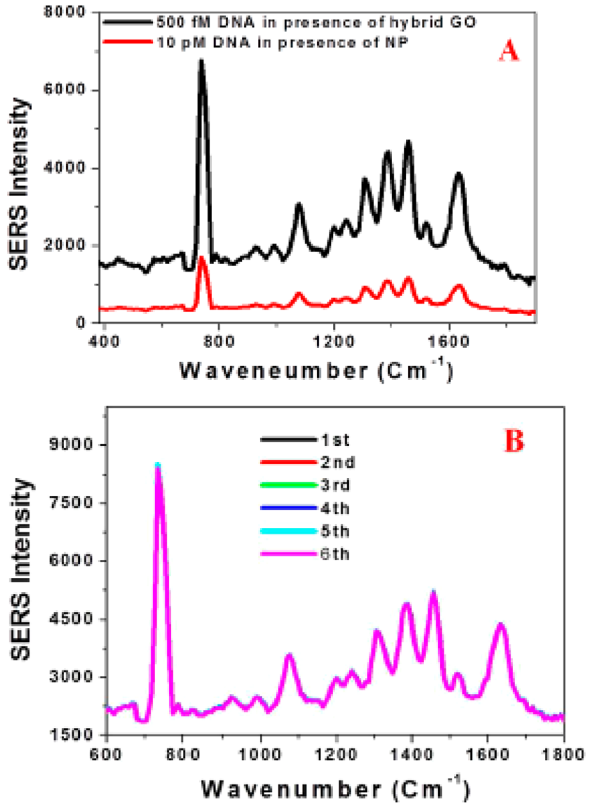

Figure 3. (A) SERS spectra of the partial sequence of the HIV-1 gag-gene, in the presence of the popcorn-shaped nanoparticle and hybrid graphene oxide. (B) SERS spectra from the partial sequence of the HIV-1 gag-gene DNA on a hybrid SERS probe made from different batches. The SERS spectrum clearly shows excellent reproducibility of our developed SERS probe.

Table 1. Raman Modes Analysis Observed from MRSA[a]

vibration mode	Raman peak position [cm^{-1}]
graphene oxide G band and amide I	1603−1615
$\delta(CH_2)$ saturated lipids	1460
graphene oxide D band	1350
$\nu(NH_2)$ Stretch for adenine and guanine	1320
ring breathing Tyr protein	855
CH_2 rock	710
C−O−C glycosidic ring deformation	580
skeletal modes CC	420

[a]We have used reported Raman bands for different microorganisms in the literature[51−53] to assign the observed bands.

biosensor applications. To monitor the reproducibility, we have obtained SERS spectra from DNA with hybrid SERS probes made from different batchs. Figure 3B clearly shows that the SERS reproducibility using our developed probe is excellent.

Next, to understand whether a hybrid SERS probe can be used for selective and sensitive label-free detection of bacteria, we have tested for the detection of MRSA. For the selective detection of MRSA, we have used an aptamer APT^{SEB1}-modified hybrid graphene oxide. Recently, it has been reported that[49] aptamer APT^{SEB1} can used for very selective detection of *Staphylococcus aureus*. Figure 4A shows that in the presence of an aptamer-modified hybrid graphene oxide, MRSA aggregated inside of the graphene oxide sheet. Figure 4B shows the SERS spectra from MRSA. Because in the MRSA the cell wall consists

dx.doi.org/10.1021/jz4020597 | J. Phys. Chem. Lett. 2013, 4, 3813−3818

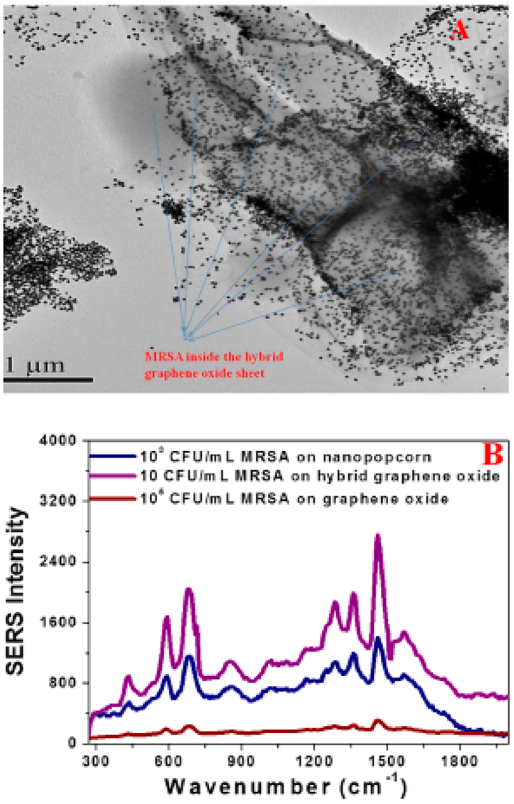

Figure 4. (A) TEM image demonstrating aggregation of MRSA bacteria inside of the nanoassemblies sheet after the addition of 1.4×10^3 cfu/mL MRSA. (B) Plot showing SERS enhancement of the Raman signal from MRSA at 670 nm excitation, in the presence of nanoassemblies. Our SERS spectra from MRSA clearly show that the detection limit can be as low as 10 MRSA.

of proteins, lipids, and carbohydrates, one can expect to see the SERS spectra from the vibrational mode of the above compositions, as shown in Figure 4B and Table 1.

SERS data observed from MRSA show $\delta(CH_2)$ saturated lipids peak at 1460 cm^{-1} and that the $\nu(NH_2)$ stretch for adenine and guanine peaks at 1320 cm^{-1}. Similarly, we have observed the ring breathing mode of the tyrosine protein peak at 855 cm^{-1}, C−O−C glycosidic ring deformation at 580 cm^{-1}, and the skeletal modes CC peak at 420 cm^{-1}. We also see D and G bands of graphene oxide. Experimentally observed SERS bands using our SERS substrate are in good agreement with the Raman bands reported for different microorganisms in the literature.[50−53] To find out the sensitivity, we have obtained MRSA concentration-dependent SERS spectra. Figure 4B clearly shows that the Raman peak can be observed even in the presence of 10 CFU/mL MRSA, which is the most sensitive reported SERS assay for the label-free detection of MRSA.

In conclusion, in this Letter, we have reported a hybrid graphene oxide based SERS probe with ultrasensitive label-fee biosensing capability. Our result demonstrates that by using a hybrid probe, Raman signals can be amplified by 11 orders of magnitudes for Rh6G by tuning both the electromagnetic and chemical effect simultaneously. Using a partial sequence of the HIV-1 gag-gene DNA, we have shown that the SERS enhancement factor for hybrid graphene oxide is about 2 orders of magnitude higher than that for only nanopopcorn. Our experimental data with different batches of hybrid graphene oxide show excellent reproducibility of the SERS signal. We have also demonstrated that the hybrid graphene oxide based SERS probe can be used for label-free MRSA identification even at the 10 CFU/mL level. Because in the hybrid probe the nanopopcorn is attached with highly chemically stable graphene oxide, our developed SERS substrate is anticipated to have a long shelf time, which will be helpful in practical applications.

MATERIALS AND EXPERIMENTS

We purchased graphite, hydrogen tetrachloroaurate, $KMnO_4$, $NaBH_4$, sodium citrate, cystamine dihydrochloride, and cetyl trimethylammonium bromide (CTAB) from Sigma-Aldrich. Aptamers were purchased from Midland Certified Reagent. MRSA bacteria were purchased from the American Type Culture Collection (ATCC, Rockville, MD). Graphene oxide attached to nanopopcorn was synthesized via a four-step process, as shown in Figure 1. The detailed synthesis procedure and characterization are discussed in the Supporting Information.

For the SERS experiment, we have used a portable SERS probe, as we have reported recently.[21−23] In brief, we have used 670 nm as an excitation light source (InPhotonics 670 nm light from a DPPS laser as the excitation light source). SERS signals were collected using a miniaturized QE65000 Ocean Optics spectrometer and data acquisition Spectra Suite spectroscopy software. For our SERS experiment, we have used 2 mW laser power for the entire experiment.

MRSA bacteria were cultured in our laboratory using the ATCC protocol as instructed. We diluted the stock bacteria of MRSA at a concentration of 10^8 CFU/mL several times to make different concentrations of bacteria. In the next step, aptamer-modified hybrid graphene oxide solutions were immersed on different concentrations of MRSA, at room temperature, before obtaining the SERS spectra.

ASSOCIATED CONTENT

Supporting Information

Detailed synthesis and characterization of the hybrid graphene oxide. This material is available free of charge via the Internet at http://pubs.acs.org.

AUTHOR INFORMATION

Corresponding Author

*E-mail: paresh.c.ray@jsums.edu. Fax: +16019793674.

Notes

The authors declare no competing financial interest.

ACKNOWLEDGMENTS

Dr. Ray thanks NSF-PREM Grant # DMR-1205194 for their generous funding.

REFERENCES

(1) Liu, J. W.; Cao, Z. H.; Lu, Y. Functional Nucleic Acid Sensors. *Chem. Rev.* **2009**, *109*, 1948−1998.

(2) Du, Y.; Li, B.; Wang, E. "Fitting" Makes "Sensing" Simple: Label-Free Detection Strategies Based on Nucleic Acid Aptamers. *Acc. Chem. Res.* **2013**, *46*, 203−213.

(3) Berkley, S.; Bertram, K.; Delfraissy, J.-F.; Draghia-Akli, R.; Fauci, A.; Hallenbeck, C.; Kagame, M. J.; Kim, P.; Mafubelu, D.; Makgoba, M. W.; et al. The 2010 Scientific Strategic Plan of the Global HIV Vaccine Enterprise. *Nat. Med.* **2010**, *16*, 981−989.

(4) Inci, F.; Tokel, O.; Wang, S. Q.; Gurkan, U. A.; Tasoglu, S.; Kuritzkes, D. R.; Demirci, U. Nanoplasmonic Quantitative Detection

of Intact Viruses from Unprocessed Whole Blood. *ACS Nano* **2013**, *7*, 4733−4745.
(5) Miranda, O. R.; Li, X.; Gonzalez, G. L.; Zhu, Z.-J.; Yan, B.; Bunz, U. H. F.; Rotello, V. M. Colorimetric Bacteria Sensing Using a Supramolecular Enzyme−Nanoparticle Biosensor. *J. Am. Chem. Soc.* **2011**, *133*, 9650−9653.
(6) Saha, K.; Agasti, S. S.; Kim, C.; Li, X.; Rotello, V. M. Gold Nanoparticles in Chemical and Biological Sensing. *Chem. Rev.* **2012**, *112*, 2739−2779.
(7) Wanunu, M.; Dadosh, T.; Ray, V.; Jin, J.; McReynolds, L.; Drndic, M. Rapid Electronic Detection of Probe-Specific MicroRNAs Using Thin Nanopore Sensors. *Nat. Nanotechnol.* **2010**, *5*, 807−814.
(8) Qian, X.; Peng, X.-H.; Ansari, D. O.; Yin-Goen, Q.; Chen, G. Z.; Shin, D. M.; Yang, L.; Young, A. N.; Wang, M. D.; Nie, S. In Vivo Tumor Targeting and Spectroscopic Detection with Surface-Enhanced Raman Nanoparticle Tags. *Nat. Biotechnol.* **2008**, *26*, 83−90.
(9) Frontiera, R. R.; Henry, A.-I.; Gruenke, N. L.; Van Duyne, R. P. Surface-Enhanced Femtosecond Stimulated Raman Spectroscopy. *J. Phys. Chem. Lett.* **2011**, *2*, 1199−1203.
(10) Kleinman, S. L.; Ringe, E.; Valley, N.; Wustholz, K. L.; Phillips, E.; Scheidt, K. A.; Schatz, G. C.; Van Duyne, R. P. Single-Molecule Surface-Enhanced Raman Spectroscopy of Crystal Violet Isotopologues: Theory and Experiment. *J. Am. Chem. Soc.* **2011**, *133*, 4115−4122.
(11) Kim, N. H.; Lee, S. J.; Moskovits, M. Aptamer-Mediated Surface-Enhanced Raman Spectroscopy Intensity Amplification. *Nano Lett.* **2010**, *10*, 4181−4185.
(12) Laurence, T. A.; Braun, G.; Talley, C.; Schwartzberg, A.; Moskovits, M.; Reich, N.; Huser, T. Rapid, Solution-Based Characterization of Optimized SERS Nanoparticle Substrates. *J. Am. Chem. Soc.* **2008**, *131*, 162−169.
(13) Barhoumi, A.; Halas, N. J. Label-Free Detection of DNA Hybridization Using Surface Enhanced Raman Spectroscopy. *J. Am. Chem. Soc.* **2010**, *132*, 12792−12793.
(14) Barhoumi, A.; Halas, N. J. Detecting Chemically Modified DNA Bases Using Surface-Enhanced Raman Spectroscopy. *J. Phys. Chem. Lett.* **2011**, *2*, 3118−3123.
(15) Brown, L. V.; Zhao, K.; King, N.; Sobhani, H.; Nordlander, P.; Halas, N. J. Surface-Enhanced Infrared Absorption Using Individual Cross Antennas Tailored to Chemical Moieties. *J. Am. Chem. Soc.* **2013**, *135*, 3688−3695.
(16) Lim, D. K.; Jeon, K. S.; Hwang, J. H.; Kim, H.; Kwon, S.; Suh, Y. D.; Nam, J. M. Highly Uniform and Reproducible Surface-Enhanced Raman Scattering from DNA-Tailorable Nanoparticles with 1-nm Interior Gap. *Nat. Nanotechnol.* **2011**, *6*, 452−460.
(17) Ji, W.; Spegazzini, N.; Kitahama, Y.; Chen, Y. J.; Zhao, B.; Ozaki, Y. pH-Response Mechanism of *p*-Aminobenzenethiol on Ag Nanoparticles Revealed by Two-Dimensional Correlation Surface-Enhanced Raman Scattering Spectroscopy. *J. Phys. Chem. Lett.* **2012**, *3*, 3204−3209.
(18) Joseph, V.; Engelbrekt, C.; Zhang, J. D.; Gernert, U.; Ulstrup, J.; Kneipp, J. Characterizing the Kinetics of Nanoparticle-Catalyzed Reactions by Surface-Enhanced Raman Scattering. *Angew. Chem., Int. Ed* **2012**, *51*, 7592−7596.
(19) Dijk, T.; Sivapalan, S. T.; DeVetter, B. M.; Yang, T. K.; Schulmerich, M. V.; Murphy, C. J.; Bhargava, R.; Carney, P. S. Competition between Extinction and Enhancement in Surface-Enhanced Raman Spectroscopy. *J. Phys. Chem. Lett.* **2013**, *4*, 1193−1196.
(20) Sivapalan, S. T.; DeVetter, B. M.; Yang, T. K.; van Dijk, T.; Schulmerich, M. V.; Carney, P. S.; Bhargava, R.; Murphy, C. J. Off-Resonance Surface-Enhanced Raman Spectroscopy from Gold Nanorod Suspensions as a Function of Aspect Ratio: Not What We Thought. *ACS Nano* **2013**, *7*, 2099−210.
(21) Dassary, S. R.; Sing, A. K.; Senapati, D.; Yu, H.; Ray, P. C. Gold Nanoparticle Based Label-Free SERS Probe for Ultrasensitive and Selective Detection of Trinitrotoluene. *J. Am. Chem. Soc.* **2009**, *131*, 13806−13812.
(22) Lu, W.; Singh, A. K.; Khan, S. A.; Senapati, D.; Yu, H.; Ray, P. C. Gold Nano-Popcorn-Based Targeted Diagnosis, Nanotherapy Treatment, and In Situ Monitoring of Photothermal Destruction Response of Prostate Cancer Cells Using Surface-Enhanced Raman Spectroscopy. *J. Am. Chem. Soc.* **2010**, *132*, 18103−18114.
(23) Singh, A. K.; Khan, S. A.; Fan, Z.; Demeritte, T.; Senapati, D.; Kanchanapally, R.; Ray, P. C. Development of a Long-Range Surface-Enhanced Raman Spectroscopy Ruler. *J. Am. Chem. Soc.* **2012**, *134*, 8662−8669.
(24) Le Ru, E. C.; Etchegoin, P. G. Single-Molecule Surface-Enhanced Raman Spectroscopy. *Annu. Rev. Phys. Chem.* **2012**, *63*, 65−87.
(25) Haran, G. Single-Molecule Raman Spectroscopy: A Probe of Surface Dynamics and Plasmonic Fields. *Acc. Chem. Res.* **2010**, *43*, 1135−1143.
(26) Willets, K. A.; Stranahan, S. M.; Weber, M. L. Shedding Light on Surface-Enhanced Raman Scattering Hot Spots through Single-Molecule Super-Resolution Imaging. *J. Phys. Chem. Lett.* **2012**, *3*, 1286−1294.
(27) Panikkanvalappil, S. R.; Mackey, M. A.; El-Sayed, M. A. Probing the Unique Dehydration-Induced Structural Modifications in Cancer Cell DNA Using Surface Enhanced Raman Spectroscopy. *J. Am. Chem. Soc.* **2013**, *135*, 4815−4821.
(28) Murphy, S.; Huang, L.; Kamat, P. V. Reduced Graphene Oxide−Silver Nanoparticle Composite as an Active SERS Material. *J. Phys. Chem. C* **2013**, *117*, 4740−4747.
(29) Ling, X.; Xie, L. M.; Fang, Y.; Xu, H.; Zhang, H. L.; Kong, J.; Dresselhaus, M. S.; Zhang, J.; Liu, Z. F. Can Graphene Be Used As a Substrate for Raman Enhancement? *Nano Lett.* **2010**, *10*, 553−561.
(30) Sun, Y. H.; Liu, K.; Miao, J.; Wang, Z. Y.; Tian, B. Z.; Zhang, L.; Li, Q. Q.; Fan, S. S.; Jiang, K. L. Highly Sensitive Surface-Enhanced Raman Scattering Substrate Made from Superaligned Carbon Nanotubes. *Nano Lett.* **2010**, *10*, 1747−1753.
(31) Thrall, E. S.; Crowther, A. C.; Yu, Z.; Brus, L. E. R6G on Graphene: High Raman Detection Sensitivity, Yet Decreased Raman Cross-Section. *Nano Lett.* **2012**, *12*, 1571−1577.
(32) Ren, W.; Fang, Y.; Wang, E. A. Binary Functional Substrate for Enrichment and Ultrasensitive SERS Spectroscopic Detection of Folic Acid Using Graphene Oxide/Ag Nanoparticle Hybrids. *ACS Nano* **2011**, *5*, 6425−6433.
(33) Saikin, S. K.; Chu, Y.; Rappoport, D.; Crozier, K. B.; Aspuru-Guzik, A. Separation of Electromagnetic and Chemical Contributions to Surface-Enhanced Raman Spectra on Nanoengineered Plasmonic Substrates. *J. Phys. Chem. Lett.* **2010**, *1*, 2740−2746.
(34) Yu, X.; Cai, H.; Zhang, W.; Li, X.; Pan, N.; Luo, Y.; Wang, X.; Hou, J. G. Tuning Chemical Enhancement of SERS by Controlling the Chemical Reduction of Graphene Oxide Nanosheets. *ACS Nano* **2011**, *5*, 952−958.
(35) Angulo, A. M.; Noguez, C.; Schatz, G. C. Electromagnetic Field Enhancement for Wedge-Shaped Metal Nanostructures. *J. Phys. Chem. Lett.* **2011**, *2*, 1978−1983.
(36) Geim, A. K; Novoselov, K. S. The Rise of Graphene. *Nat. Mater.* **2007**, *6*, 183−191.
(37) Lightcap, I. V.; Kamat, P. V. Graphitic Design: Prospects of Graphene-Based Nanocomposites for Solar Energy Conversion, Storage, and Sensing. *Acc. Chem. Res.* **2013**, *46*, 2235−2243.
(38) Kamat, P V Graphene-Based Nanoarchitectures. Anchoring Semiconductor and Metal Nanoparticles on a Two-Dimensional Carbon Support. *J. Phys. Chem. Lett.* **2010**, *1*, 520−527.
(39) Li, X.; Wang, X.; Zhang, L.; Lee, S.; Dai, H. Chemically Derived, Ultrasmooth Graphene Nanoribbon Semiconductors. *Science.* **2008**, *319*, 1229−1232.
(40) Gao, W.; Alemany, L. B.; Ci, L.; Ajayan, P. M. New Insights into the Structure and Reduction of Graphite Oxide. *Nat. Chem.* **2009**, *1*, 403−408.
(41) Hossain, M. Z.; Johns, J. E.; Bevan, K. H.; Karmel, H. J.; Liang, Y. T.; Yoshimoto, S.; Mukai, K.; Koitaya, T.; Yoshinobu, J.; Kawai, M.; Lear, A. M.; Kesmodel, L. L.; Tait, S. L.; Hersham, M. C. Chemically

Homogeneous and Thermally Reversible Oxidation of Epitaxial Graphene. *Nat. Chem.* **2012**, *4*, 305−309.
(42) Dreyer, D. R.; Park, S.; Bielawski, C. W.; Ruoff, R. S. The Chemistry of Graphene Oxide. *Chem. Soc. Rev.* **2010**, *39*, 228−240.
(43) Lightcap, I. V.; Kosel, T. H.; Kamat, P. V. Anchoring Semiconductor and Metal Nanoparticles on a Two-Dimensional Catalyst Mat. Storing and Shuttling Electrons with Reduced Graphene Oxide. *Nano Lett.* **2010**, *10*, 577−583.
(44) Bagri, A.; Mattevi, C.; Acik, M.; Chabal, Y. J.; Chhowalla, M.; Shenoy, V. B. Structural Evolution during the Reduction of Chemically Derived Graphene Oxide. *Nat. Chem.* **2010**, *2*, 581−587.
(45) Zhu, Y.; Sun, Z.; Yan, Z.; Jin, Z.; Tour, J. M. Rational Design of Hybrid Graphene Films for High Performance Transparent Electrodes. *ACS Nano* **2011**, *5*, 6472−6479.
(46) Robinson, J. T.; Tabakman, S. M.; Liang, Y.; Wang, H.; Casalongue, S. H.; Vinh, D.; Dai, H. Ultrasmall Reduced Graphene Oxide with High Near-Infrared Absorbance for Photothermal Therapy. *J. Am. Chem. Soc.* **2011**, *133*, 6825−6831.
(47) Liu, Z.; Robinson, J. T.; Sun, X.; Dai, H.; Wang, Y.; Li, Z.; Hu, D.; Lin, C.-T.; Li, J.; Lin, Y. Aptamer/Graphene Oxide Nanocomplex for In Situ Molecular Probing in Living Cells. *J. Am. Chem. Soc.* **2010**, *132*, 9274−9276.
(48) Hummers, W. S.; Offeman, R. E. Preparation of Graphitic Oxide. *J. Am. Chem. Soc.* **1958**, *80*, 1339−1339.
(49) Mei, Q.; Zhang, K.; Guan, G.; Liu, B.; Wang, S.; Zhang, Z. Highly Efficient Photoluminescent Graphene Oxide with Tunable Surface Properties. *Chem. Commun.* **2010**, *46*, 7319−7321.
(50) Dwivedi, H. P.; Smiley, R. D.; Jaykus, L. A. Selection of DNA Aptamers for Capture and Detection of Salmonella Typhimurium Using a Whole-Cell SELEX Approach in Conjunction with Cell Sorting. *Appl. Microbiol. Biotechnol.* **2013**, *97*, 3677−86.
(51) Khan, S. A.; Singh, A. K.; Senapati, D.; Fan, Z.; Ray, P. C. Nanomaterial for Targeted Detection and Photothermal Killing of Bacteria. *Chem. Soc. Rev.* **2012**, *41*, 3193−3209.
(52) Premasiri, W. R.; Moir, D. T.; Klempner, M. S.; Krieger, N.; Jones, G.; Ziegler, L. D. Characterization of the Surface Enhanced Raman Scattering (SERS) of Bacteria. *J. Phys. Chem. B* **2005**, *109*, 312−320.
(53) Wang, Y.; Lee, K.; Irudayaraj, J. Silver Nanosphere SERS Probes for Sensitive Identification of Pathogens. *J. Phys. Chem. C* **2010**, *114*, 16122−16128.